

THE SYNERGY OF GAMMA-RAY BURST DETECTORS IN THE GLAST ERA

David L. Band, on behalf of the GLAST collaboration

*CRESST and Code 661, NASA/Goddard Space Flight Center, Greenbelt, MD 20771
CSST, University of Maryland, Baltimore County, 1000 Hilltop Circle, Baltimore, MD 21250*

Abstract. Simultaneous observations by the large number of gamma-ray burst detectors operating in the GLAST era will provide the spectra, lightcurves and locations necessary for studying burst physics and testing the putative relations between intrinsic burst properties. The detectors' energy band and the accumulation timescale of their trigger system affect their sensitivity to hard vs. soft and long vs. short bursts. Coordination of the Swift and GLAST observing plans consistent with Swift's other science objectives could increase the detection rate of GLAST bursts with redshifts.

Keywords: gamma-ray burst detectors

PACS: 95.55.-n,95.55.Ka

Anticipated to be launched in spring, 2008, the Gamma-ray Large Area Space Telescope (GLAST) will join a large number of gamma-ray burst detectors that are already operating in space. The strengths of these different detectors complement each other, both in providing capabilities that are absent in other detectors and in allowing cross-calibration. In this work I compare the different detectors and their capabilities.

The Table lists burst detectors that will operate during the first few years of the GLAST mission. Quantitative comparisons between different missions are difficult because of the operational details. For example, the sensitivity usually varies across a detector's field-of-view (FOV), resulting in a burst detection threshold that is not uniform. Because many detectors can provide spectra over a larger energy band than used for the burst triggers, I provide two energy bands in the Table.

Burst triggers ultimately compare an increase in the number of detected counts in an energy band ΔE and accumulation time Δt to the expected background fluctuations; the burst threshold is derived from the signal-to-noise ratio for a $\Delta E - \Delta t$ bin. The burst detection sensitivity is the threshold flux F_T (here over the 1–1000 keV band) as a function of the burst spectrum (here over 1 s). Burst spectra can be parameterized by the 'Band' function,[1] characterized by low and high energy spectral indices α and β , and a characteristic energy E_p , the photon energy of the peak of the $E^2 N(E) \propto \nu f_\nu$. The Figure's left hand panel presents F_T as a function of E_p , fixing $\alpha = -1/2$ and $\beta = -2$, for different burst detectors. Note that this figure does not show a detector's sensitivity at a given energy but instead the detector sensitivity to a burst with a given E_p . Here I show the sensitivity for $\Delta t = 1$, but detector triggers operate with a variety of Δt values, and differ in their sensitivity to bursts with different durations.[2, 7]

In many cases we are not interested in whether a detector detects a burst—spectral data may be available regardless of whether the detector triggered—but in the spectra the detector accumulates. The Figure's right hand panel shows the detectors' spectral

TABLE 1. Burst Detectors in GLAST Era

Mission-Detector	Orbit	FOV*	A_{eff} cm	σ^\dagger	ΔE spec.**	ΔE trig.‡	Δt	Ref.
GLAST-LAT§	565 km, $\iota=25.3^\circ$	~ 3.5	8000	0.1°	25 MeV–300 GeV	25 MeV–300 GeV	Variable	[3]
GLAST-GBM¶	565 km, $\iota=25.3^\circ$	~ 9	122×12	8°	8 keV–30 MeV	50–300 keV	0.064–4 s	[4]
Swift-BAT	590 km $\iota=20.1^\circ$	~ 1.4	2600	$4'$	15–150 keV	15–150 keV	0.004–64 s	[5, 6, 7]
Konus-Wind††	L1	$\sim 4\pi$	133×2	—	12 keV–10 MeV	45–190 keV	0.15, 1 s	[8, 9]
Suzaku-WAM‡‡	570 km, $\iota=31^\circ$	$\sim 4\pi$	800×4	—	50 keV–5 MeV	110–240 keV	0.25, 1 s	[10]
RHESSI	580 km, $\iota=38^\circ$	$\sim 4\pi$	~ 150	—	>50 keV	>50 keV	Variable	[11]
Super-AGILE§§	~ 580 km, $\iota < 3^\circ$	1.4	312×4	$1.5'$	15–45 keV	15–45 keV	Variable	[12, 13]
AGILE Mini-Cal	~ 580 km, $\iota < 3^\circ$	~ 2.5	~ 1400	—	300 keV–100 MeV	300 keV–100 MeV	Variable	[14, 13]
AGILE TKR	~ 580 km, $\iota < 3^\circ$	~ 2.5	~ 1000	$15'$	30 MeV–50 GeV	30 MeV–50 GeV	Variable	[13]
INTEGRAL ISGRI/IBIS¶¶	Ecc.	0.1	1300	$2'$	15 keV–1 MeV	15 keV–1 MeV	8ms–40 s	[15, 16]
INTEGRAL SPI***	Ecc.	0.1	250	$10'$	20 keV–8 MeV	—	—	[17]
INTEGRAL SPI ACS†††	Ecc.	$\sim 4\pi$	~ 3000	—	—	—	> 50 ms	[15, 16]

* Field-of-view, in steradians.

† Typical localization uncertainty.

** Energy band for spectroscopy.

‡ Energy band for burst trigger.

§ The LAT FOV is the total sky region from which events are accepted, and this definition does not account for sensitivity variations over this area. The effective area given is the value above ~ 3 GeV. The localization depends strongly on the burst intensity and spectrum; a typical uncertainty for a strong burst is shown. Both onboard and ground triggers will be used. The LAT will also observe GeV band afterglows.

¶ The FOV is down to the horizon. The onboard localization uncertainty is shown; the ground processing will reduce the uncertainty.

|| The mask open fraction is applied to the effective area. Note that XRT and UVOT reduce location uncertainties to arcsecond scale. The XRT and UVOT will observe the optical through X-ray afterglows.

†† Two scintillation detectors pointing in opposite directions; the sensitivity is low in the plane perpendicular to the detector axes.

‡‡ Four scintillating slabs; the sensitivity is low in the plane of the slabs.

§§ FOV used is coded in both x and y directions

¶¶ The effective area includes the mask opacity. FOV is within the FWHM.

*** The effective area includes the mask opacity.

††† The BGO shields of the SPI cannot localize bursts.

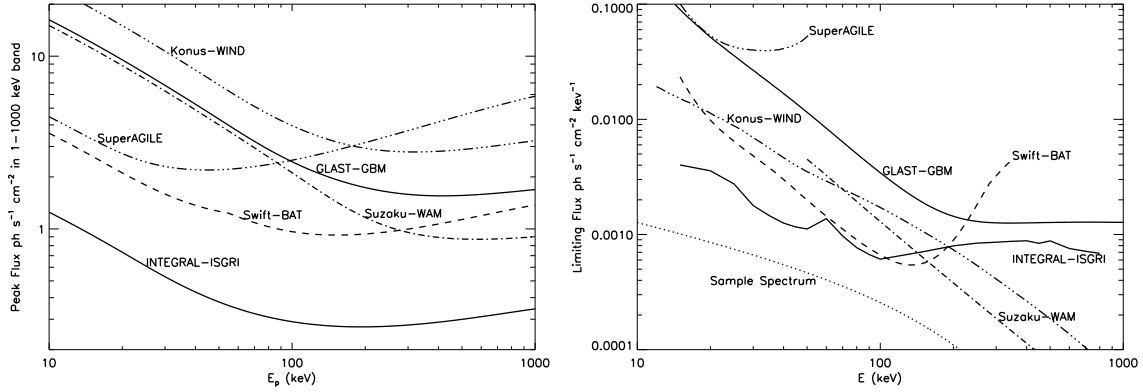


FIGURE 1. Left: Threshold 1–1000 keV flux as a function of E_p for different detectors assuming $\alpha = -1/2$, $\beta = -2$ and $\Delta t=1$ s. Right: Spectral sensitivity, the flux necessary at E for a 3σ measurement in 1 s in a band of width $\Delta E/E = 1/2$.

sensitivity, the continuum sensitivity over a 1 s accumulation time.

The synergy between missions will be maximized by simultaneous burst observations. Particularly important is the overlap between detectors with spectral capability (GLAST, Konus-Wind, Suzaku-WAM) and localization capability (Swift-BAT and INTEGRAL-ISGRI). Konus-Wind and INTEGRAL SPI-ACS essentially see the entire sky, while GLAST-GBM, Suzaku-WAM and RHESSI see down to the horizon for a low-Earth orbit. Although ISGRI is sensitive, it has a (relatively) small FOV. The GLAST instruments—the LAT (<20 MeV– >300 GeV) and the GBM (8 keV–30 MeV)—have large FOVs and the GLAST observatory will operate in a fixed survey mode. Swift-BAT also has a large FOV and Swift has a very flexible observing timeline.

Because of their large FOVs and complementary strengths—localizing bursts and following afterglows for Swift, accumulating spectra over 7 energy decades for GLAST—increasing the overlap between these two missions will have major scientific gains. During most of its mission, the LAT’s pointing will follow a fixed pattern to execute an all-sky survey. On the other hand, Swift observes a number of targets each orbit with its Narrow Field Instruments (NFIs)—X-ray Telescope (XRT) and Ultraviolet-Optical Telescope (UVOT); the wide FOV Burst Alert Telescope (BAT), which observes bursts’ prompt emission, is centered on the NFIs. The NFI targets are burst afterglows and other astrophysically interesting sources. Semi-analytic calculations show that if Swift does not coordinate its pointings with GLAST, $\sim 13\%$ of GLAST-LAT bursts will be in the Swift-BAT FOV, and $\sim 27\%$ of Swift-BAT bursts in the GLAST-LAT FOV. If Swift points as close as possible to the LAT pointing direction these overlap numbers could increase by $\sim 3\times$! However, this estimate neglects Swift’s observational constraints, and sacrifices many of Swift’s scientific objectives. Nonetheless, the judicious choice of Swift NFI targets could increase the LAT-BAT overlap by $\sim 2\times$. For example, Swift’s timeline could include two sets of targets, one observed when the LAT is pointed towards the northern hemisphere, and the second for the southern hemisphere. Procedures to increase this overlap with little impact on Swift’s science objectives are under development. An increase in the LAT-BAT overlap would of necessity increase the GBM-BAT

overlap. Note that a burst in a detector's FOV may nonetheless be too faint to be detected.

Coordination with GLAST of the timelines of most of the other burst missions would yield meagre increases in the detector overlaps because the detectors are nearly all-sky (or are occulted by the Earth), or their operations do not lend themselves to such coordination. Because of the different FOVs and the varying detection sensitivities, I foresee that most bursts detected by one of the constellation of burst detectors will have at best upper limits from other detectors. A few bursts a year will be well-observed by a varying assortment of missions; for example, Swift might provide a location, Konus-Wind spectra, and Swift and GLAST-LAT afterglow observations. If the Swift timeline is coordinated with GLAST, then the LAT and BAT will observe simultaneously ~ 50 bursts a year, although the LAT will probably detect less than half of these. The localizations, spectra and lightcurves of this last set of bursts will advance the study of gamma-ray bursts.

ACKNOWLEDGMENTS

I thank members of the BAT team at GSFC and of the GLAST GRB working group for insightful discussions.

REFERENCES

1. D. Band, et al., *Ap.J.* **413**, 281–292 (1993).
2. D. Band, *Ap.J.* **588**, 945 (2003).
3. N. Omodei, and J. Norris, “LAT observation of GRBs: Simulations and Sensitivity studies”, in *AIPC 921*, edited by S. Ritz, P. Michelson, and C. A. Meegan, pp. 472–475 (2007).
4. C. Meegan, et al., “The GLAST Burst Monitor”, in *AIPC 921*, edited by S. Ritz, P. Michelson, and C. A. Meegan, pp. 13–18 (2007).
5. N. Gehrels, et al., *Ap.J.* **611**, 1005–1020 (2004).
6. S. D. Barthelmy, et al., *Space Science Reviews* **120**, 143–164 (2005).
7. D. L. Band, *Ap.J.* **644**, 378–384 (2006).
8. R. L. Aptekar, et al., *Space Science Reviews* **71**, 265–272 (1995).
9. E. P. Mazets, et al., “Konus catalog of short GRBs”, in *ASPC 312*, edited by M. Feroci, F. Frontera, N. Masetti, and L. Piro, pp. 102–105 (2004).
10. K. Yamaoka, et al., “In-orbit performance of the Suzaku wideband all-sky monitor”, in *Space Telescopes and Instrumentation II: Ultraviolet to Gamma Ray*. Edited by Turner, Martin J. L.; Hasinger, Günther. Proceedings of the SPIE, Volume 6266, pp. 626643 (2006).
11. C. Wigger, et al., *ArXiv e-prints* **704** (2007), 0704.3038.
12. E. Costa, et al., “Super-agile-The X-ray detector for the gamma-ray mission agile”, in *AIPC 599*, edited by N. E. White, G. Malaguti, and G. G. C. Palumbo, pp. 582–585 (2001).
13. M. Tavani, et al., “The AGILE mission and its scientific instrument”, in *Space Telescopes and Instrumentation II: Ultraviolet to Gamma Ray*. Edited by Turner, Martin J. L.; Hasinger, Günther. Proceedings of the SPIE, Volume 6266, pp. 626603 (2006).
14. C. Labanti, et al., “The mini-calorimeter of the AGILE satellite”, in *Space Telescopes and Instrumentation II: Ultraviolet to Gamma Ray*. Edited by Turner, Martin J. L.; Hasinger, Günther. Proceedings of the SPIE, Volume 6266, pp. 62663Q (2006).
15. F. Lebrun, et al., *A&A* **411**, L141–L148 (2003).
16. S. Mereghetti, and D. Götz, *Nuovo Cimento C Geophysics Space Physics C* **28**, 259 (2005).
17. A. V. Kienlin, N. Arend, G. Lichti, A. Strong, and P. Connell, “Gamma-Ray Burst Detection with INTEGRAL/SPI,” in *ASPC 312*, edited by M. Feroci, F. Frontera, N. Masetti, and L. Piro, 2004, p. 551.